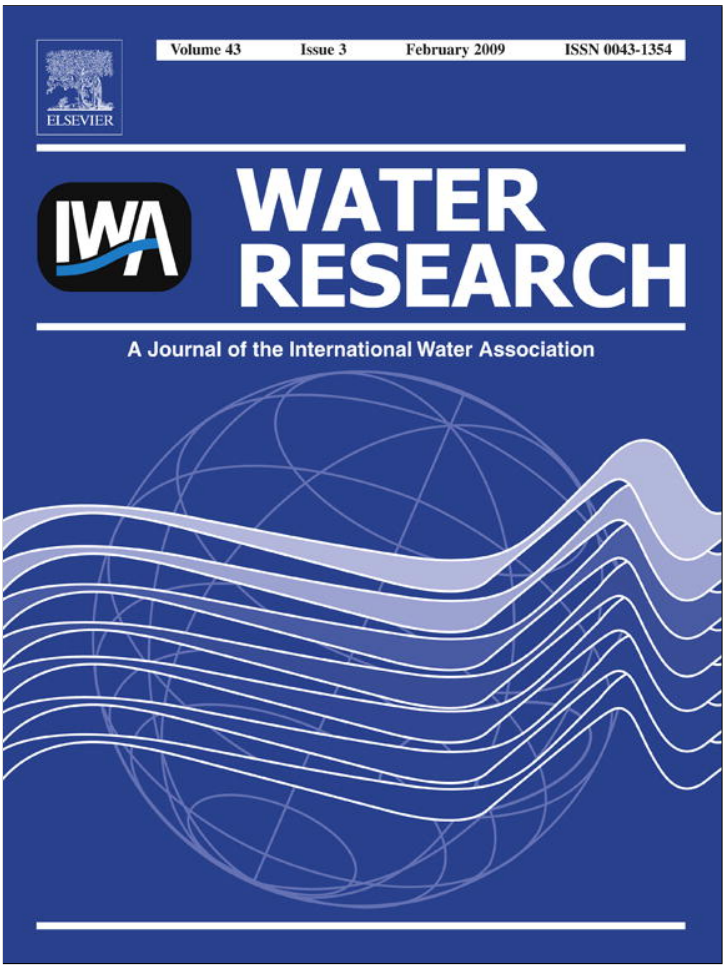

WATER RESEARCH 43 (2009) 715–723

Available at www.sciencedirect.com

ScienceDirect

journal homepage: www.elsevier.com/locate/watres

Polysulfone ultrafiltration membranes impregnated with silver nanoparticles show improved biofouling resistance and virus removal

*Katherine Zodrow, Léna Brunet, Shaily Mahendra, Dong Li, Anna Zhang, Qilin Li, Pedro J.J. Alvarez**

Department of Civil and Environmental Engineering, Rice University, 6100 Main Street, Houston, TX 77005, USA

ARTICLE INFO

Article history:
Received 30 August 2008
Received in revised form
29 October 2008
Accepted 5 November 2008
Published online 24 November 2008

Keywords:
Nanosilver
Water filtration membranes
Biofouling
Virus removal

ABSTRACT

Biofouling and virus penetration are two significant obstacles in water treatment membrane filtration. Biofouling reduces membrane permeability, increases energy costs, and decreases the lifetime of membranes. In order to effectively remove viruses, nanofiltration or reverse osmosis (both high energy filtration schemes) must be used. Thus, there is an urgent demand for low pressure membranes with anti-biofouling and antiviral properties. The antibacterial properties of silver are well known, and silver nanoparticles (nAg) are now incorporated into a wide variety of consumer products for microbial control. In this study, nAg incorporated into polysulfone ultrafiltration membranes (nAg–PSf) exhibited antimicrobial properties towards a variety of bacteria, including *Escherichia coli* K12 and *Pseudomonas mendocina* KR1, and the MS2 bacteriophage. Nanosilver incorporation also increased membrane hydrophilicity, reducing the potential for other types of membrane fouling. XPS analysis indicated a significant loss of silver from the membrane surface after a relatively short filtration period (0.4 L/cm^2) even though ICP analysis of digested membrane material showed that 90% of the added silver remained in the membrane. This silver loss resulted in a significant loss of antibacterial and antiviral activity. Thus, successful fabrication of nAg-impregnated membranes needs to allow for the release of sufficient silver ions for microbial control while preventing a rapid depletion of silver.

1. Introduction

The reliability and ease of operation of membrane-based water filtration systems have led to their increasing use in water and wastewater treatment. However, biofouling of these membranes, including microbial release of extracellular polymeric substances (EPS), and the associated decrease in membrane flux, increases energy costs and shortens membrane life (Mcdonogh et al., 1994). Certain membrane characteristics affect the likelihood of biofouling, including surface charge and hydrophobicity (Ridgway et al., 1999), and membrane biofouling is commonly controlled with pretreatment (coagulation) or with chemical cleaning (e.g., chlorine) during backwash. Although pretreatment can be an effective form of biofouling control, many polymeric membranes cannot withstand the corrosiveness of chemical cleaners.

The use of microfiltration and ultrafiltration to remove viruses from water and wastewater is limited by the small size

* *Corresponding author*. Tel.: +1 713 348 5903; fax: +1 713 348 5203.
E-mail address: alvarez@rice.edu (P.J.J. Alvarez).
0043-1354/$ – see front matter © 2008 Elsevier Ltd. All rights reserved.
doi:10.1016/j.watres.2008.11.014

of viruses and the relatively large pore size of the membranes (Zhu et al., 2005). Also, membrane surface imperfections can increase the possibility of virus penetration during filtration (Bellara et al., 1998). Thus, organic microfiltration and ultrafiltration membranes seldom experience effective virus removal without particular pretreatment or post-treatment procedures.

For millennia people have taken advantage of the antimicrobial properties of silver, employing methods as simple as storing drinking water and milk in silver containers and as complex as silver-coating medical implants and instruments (Davies and Etris, 1997; Bosetti et al., 2002; Li et al., 2008). The lower thresholds for silver ion (Ag^+) toxicity lie between 0.01 and 0.1 mg/L (Ratte, 1999; Cunningham et al., 2008), while the World Health Organization established that 0.1 mg/L of silver in drinking water can be tolerated without risk to human health (WHO, 2004). This guideline is set to prevent argyria from 70-year cumulative dose of 10 g (one-half of the human no observable adverse effect level, NOAEL). In humans, silver ions cannot cross the blood–brain barrier, and are regulated by blood metallothioneins, which bind it in metal-thiolate-cluster structures for transport, storage, and detoxification (Davies and Etris, 1997).

The antibacterial mechanism of silver is related to its interaction with sulfur and phosphorus, most notably thiol groups (S–H) present in cysteine and other compounds (Davies and Etris, 1997). Interaction of ionic silver (which can be released from nAg) with thiol groups and formation of S–Ag or disulfide bonds can damage bacterial proteins, interrupt the electron transport chain, and dimerize DNA (Trevors, 1987; Russell and Hugo, 1994; Feng et al., 2000). Similarly, the antiviral properties of silver ions involve interaction with viral DNA and thiol groups in proteins (Kim et al., 2008).

Silver nanoparticles may damage some bacterial cells and viruses by mechanisms other than the release of silver ions. For example, HIV-1 viruses were inhibited from binding to host cells by nAg particles ranging from 1 to 10 nm that preferentially bound to viral gp120 glycoproteins (Elechiguerra et al., 2005). In other studies, damage to the cell wall of nAg-exposed bacteria was visually apparent, and cell death was suspected to be due to an increase in cell membrane permeability that lead to osmotic collapse and a release of intracellular material (Sondi and Salopek-Sondi, 2004; Morones et al., 2005; Panacek et al., 2006). The toxicity of nAg to bacteria is greatly influenced by nAg particle size and shape. While nAg synthesis and uptake in bacteria have been reported for spheres and rods up to 80 nm (Pal et al., 2007), particles in the range of 1–10 nm with high density <111> facets are most likely to interact negatively with the cell (Xu et al., 2004; Morones et al., 2005; Gogoi et al., 2006; Pal et al., 2007). The toxicity mechanisms of Ag^+ ions that dissolve from nAg are well understood, but the extent to which direct contact between bacteria and nAg causes toxicity remains unclear.

Incorporation of antimicrobial nanomaterials into membranes offer an innovative potential solution to biofouling control (Savage and Diallo, 2005; de Prijck et al., 2007; Li et al., 2008), and silver ions and nAg have been studied for a wide variety of water treatment processes, including water filtration membranes. Nanosilver has been incorporated into cellulose acetate (Chou et al., 2005), polyimide (Deng et al., 2008), polyamide (Damm et al., 2007), and poly(2-ethyl-2-oxazoline) (Kang et al., 2006) membranes. However, the long-term effectiveness of the incorporated nAg in preventing biofouling during continuous filtration has not been addressed. Furthermore, little research has been conducted on the incorporation of nAg in polysulfone membranes, which are notable for their widespread application in water filtration (in microfiltration, ultrafiltration, and occasionally, nanofiltration membranes). This motivated the experiments presented herein, which address the antimicrobial and antiviral properties of polysulfone membranes impregnated with nAg and their application for biofouling and virus control.

2. Methods

2.1. Membrane fabrication

Polysulfone ultrafiltration membranes were made using the wet phase-inversion process (Mulder, 1990). First, poly(vinyl pyrrolidone) (PVP, MW: 55,000; Sigma–Aldrich) was dissolved in the solvent *N*-methyl-2-pyrrolidone (NMP, 99.5%; Sigma–Aldrich) at 50 °C with stirring. Silver nanoparticles (1–70 nm; Novacentrix, Austin, Texas) were added and dispersed with a sonicating probe (Fisher Scientific Sonic Dismembrator Model 100). The solution was heated to 120 °C, and polysulfone (PSf, Udel P3500; Solvay Membranes) was added. The final solution was composed of 15% PSf, 10% PVP, 75% NMP, and 0.22% nAg by weight. After the solution was cooled, a thin film of the casting solution was deposited onto a glass plate using an aluminum casting knife. The glass plate and membrane film were quickly transferred to a water bath at room temperature for the remainder of the phase-inversion process.

2.2. Membrane characterization

Membrane permeability was determined from clean water flux measurement using deionized water at room temperature and a Sterlitech dead-end filtration cell over a pressure range of 0.34–14 bars. Before the permeability measurement, the membrane was compacted at a pressure of 14 bars. Hydrophobicity of the membranes was determined by sessile drop contact angle measurement of water on membranes that were dried overnight (DROPImage Standard). Membrane surface zeta potential was measured to determine whether incorporation of nAg changes membrane surface properties. Streaming potential measurement was conducted in a 10^{-2} M NaCl background solution (a concentration similar to that used in bacterial experiments) at pH 5, 7, and 9 (ZetaCAD, CAD Instrumentation; Les Essarts Le Roi, France) (Fievet et al., 2003). Images of dried membrane cross-sections were taken with a scanning electron microscope (FEI Quanta 400 ESEM FEG, 20 kV) in high vacuum mode after coating with approximately 10 nm of gold (CrC-150 Sputtering System, TORR International) to observe membrane asymmetry and pore structure. To measure silver content, the membrane was digested by sonication in 2% HNO_3 (Branson Ultrasonic 5510; Danbury, CT) for 3 days. After digestion, the suspension was filtered through a 1 μm-pore-size glass fiber filter

(Gelman, Type E) to remove large particles, and analyzed for total silver content. Total silver recovery by this method was 104% ± 0.3% ($n = 3$).

Total silver concentrations were quantified using a Perkin-Elmer (Norwalk, CT) Optima 4300 DV Inductively Coupled Plasma-Optical Emission Spectrometer (ICP-OES). All measurements were carried out in the axial mode at 328.068 nm. Yttrium (371.029 nm) was used as an internal standard for calibration as recommended by the ICP manufacturer. All samples and ICP standards were acidified by 0.5% trace metal grade HNO_3. The detection limit of silver for the ICP was 0.01 mg/L.

Analysis of silver present on the surface of the membrane was conducted using X-Ray Photoelectron Spectroscopy (PHI Quantera XPS). Volumes of 1 and 4 L of deionized (DI) water were filtered through nAg–PSf membranes with a vacuum filtration cell. The membranes were dried thoroughly before analysis. A detailed scan for silver was conducted at a range of 362–385 eV.

2.3. Analysis of silver in the filtrate

Four liters of deionized (DI) water were filtered with a vacuum filtration cell, and the total silver concentrations in the filtrate were quantified using ICP as described above. Silver leaching mainly in ionic form was confirmed by TEM analysis (JEM FasTEM 2010; 200 kV accelerating voltage), as the mass of silver recovered in nanoparticle form accounted for less than 10^{-7} percent of the silver in the filtrate. For this analysis, five drops of filtrate (5 μL) were placed on a carbon grid (Type A, 300 mesh; Ted Pella, Inc.; Redding, CA, USA). Each drop was allowed to dry thoroughly before the next drop was applied. For the mass balance, it was assumed that the density of nAg was equivalent to that of metallic silver (i.e., 10.5 g/cm^3) (Kaye and Laby, 1986). The size and number of silver particles were determined with ImageJ (National Institute of Health).

2.4. Antibacterial properties of nAg membranes

To assess initial effectiveness of the antibacterial properties of the membranes, 3 mL of stationary phase *Escherichia coli* K12 (American Type Culture Collection, ATCC, 25404) was serially diluted to 10 CFU/mL from a stock of 10^9 CFU/mL (OD_{600} 1–1.5, measured by Ultrospec 2100 Pro, Amersham Biosciences) in Minimal Davis (MD) medium (0.7 g/L K_2HPO_4, 0.2 g/L KH_2PO_4, 1 g/L $(NH_4)_2SO_4$, 0.5 g/L Na-citrate, 0.1 g/L $MgSO_4 \cdot 7H_2O$) and was filtered onto sterile PSf and nAg–PSf membranes using a vacuum filtration cell (both the membranes and the filtration cell were previously autoclaved at 121 °C for 15 min). Membranes were then placed on Luria–Bertani (LB) agar plates and incubated at 35 °C overnight. Colony forming units (CFU) on the membrane surface were counted on the following day, giving the total number of viable cells after filtration and incubation.

The antibacterial contribution from silver contained in the membrane was evaluated with the use of the amino acid cysteine (Sigma; St. Louis, Missouri, USA). Cysteine forms complexes with Ag^+ released from nAg, making Ag^+ ions unavailable to act as an antimicrobial agents (Silver and Phung, 1996; Liau et al., 1997). However, full discernment of the antibacterial role of Ag^+ may not be possible with this approach because cysteine may also bind to nAg particles and reduce their bioavailability, which confounds the interpretation of decreased toxicity attributable solely to Ag^+ complexation. Batch growth experiments were performed with *E. coli* K12 in MD with 1 g/L glucose in the presence of cysteine. After two hours of incubation, the suspension was spiked with 2.7 mg/L nAg. The optical density at 600 nm was monitored (Ultrospec 2100 Pro, Amersham Biosciences) as an indicator of bacterial growth.

2.5. Biofouling resistance in nAg membranes

The attachment of bacteria to the membrane surface was assessed with *E. coli* in MD medium. Stationary phase bacteria (~10^9 CFU/mL) were incubated with 1-cm^2 PSf and nAg–PSf membrane coupons at 35 °C while shaking for 4 h. This incubation time resulted in a visible layer of attached bacteria with low enough cell colony density to remain countable. The membranes were removed from the media and rinsed gently with sterile deionized water thrice. Bacteria on the membrane, specifically the nucleic acids, were stained with 1 μg/mL 4′,6-diamidina-2-phenylidole (DAPI) for 5 min and then rinsed. Membrane coupons were mounted to a glass slide and viewed with a fluorescence microscope (Zeiss Axioplan, MetaMorph Software). DAPI showed little background fluorescence on membranes that had not been exposed to bacteria. Cells were enumerated with the software ImageJ (National Institute of Health) and cell density on the membrane was calculated.

The potential of biofilm formation on the membrane surface was evaluated using the method described by de Prijck et al. (2007). Briefly, stationary phase cultures of *Pseudomonas mendocina* KR1, a prolific biofilm forming bacterium (Jayasekara et al., 1999), were diluted to OD_{600} 10^{-6} (10^3 cells/mL) and incubated with a sterile membrane coupon (PSf and nAg–PSf) in 5 mL of MD media for 24, 48, and 72 h. Both the planktonic cells in the supernatant and the sessile cells in the biofilm were counted. To enumerate the planktonic cells, three- to five-fold dilutions were plated onto LB agar plates and incubated overnight. Colony forming units (CFU) were counted the following day. To measure the number of cells attached to the membrane, the membranes were removed from the media and rinsed with sterile DI water. The membranes were placed in 2 mL of fresh MD media, vortexed (Vortex Genie 2, VWR Scientific) on the highest setting for 30 s and placed in a sonication bath for 30 s. This biofilm disruption procedure was performed twice. Samples were taken directly from the supernatant, deposited on a LB agar plate, and incubated overnight. The CFU on the plates were then counted. The influence of cysteine (used as Ag^+ ligand) on biofilm growth on the nAg–PSf membrane was measured similarly, but in the presence of 27 mg/L cysteine. This concentration was chosen to assure a surplus of cysteine to chelate silver present in the membrane. In order to examine the effectiveness of nAg impregnation to control of silver-resistant bacteria, biofouling experiments were repeated with *Pseudomonas aeruginosa* (ATCC 700829) harboring metal resistance *czc* genes (Hassen et al., 2001), with an initial concentration of 10^7 cells/mL.

2.6. Antiviral properties of nAg membranes

Bacteriophage MS2 (ATCC 15597-B1) was propagated according to a previously published method (Zhu et al., 2005) with minor modifications. Initial concentrations of MS2 phage in the range of 10^4–10^5 plaque-forming units per milliliter (PFU/mL) suspended in 2 mL 0.1 M bicarbonate buffer were filtered through the nAg–PSf and control PSf membranes. Virus concentrations were assayed using an agar-overlay technique (Kennedy et al., 1986). Briefly, 100 μL aliquots of influent or filtrate were serially diluted in 900 μL bicarbonate buffer, and incubated with 100 μL stationary phase MS2 host *E. coli* (ATCC 15597) for 10 min. This mixture was added to 3 mL warm (45 °C) tryptic soy soft agar, overlaid upon Luria–Bertani agar plates, and incubated at 37 °C. Plaques were counted after 24 h, and removal was calculated as logarithm of the ratio of PFUs in the filtrate to those in the influent.

3. Results and discussion

3.1. Membrane characterization

Membranes impregnated with 0.9% (by weight) nAg (nAg–PSf) had similar permeability and surface charge to the control membrane without nAg (PSf) (Table 1). The permeability of both membranes was typical of ultrafiltration membranes (Cheryan, 1998). The nAg membrane was significantly more hydrophilic than the control ($p < 0.05$), with a contact angle 10% smaller than that of the PSf membrane. This decrease in hydrophobicity can be potentially beneficial in preventing chemical fouling, but is beyond the scope of this study and will not be discussed here. Cross-section images of the membrane showed very similar morphologies. The asymmetry of the membrane was apparent and the addition of nAg to the membrane did not visibly alter the membrane structure (Fig. 1).

3.2. Analysis of silver in the filtrate

The leaching of Ag^+ was confirmed by ICP and TEM analyses. Concentrations of Ag^+ as high as 0.034 mg/L were found in the membrane permeate that was filtered at a rate of 0.004 mL/cm^2/s. The Ag^+ concentration in the filtrate decreased as more water was filtered, and after approximately 0.31 L/cm^2 of filtration, no more silver was detected in the filtrate. TEM analysis of a concentrated solution of the filtrate revealed that the silver leached from the membrane was predominantly in ionic form. Although a few nAg particles were observed in the filtrate, these particles accounted for less than 10^{-7} percent of the total silver concentration of the filtrate. XPS analysis of the membrane indicated that silver was nearly depleted from the membrane surface after 0.4 L/cm^2 of filtration (Fig. 2), even though ICP analysis of the digested membrane indicated that 90% of the added silver remained within the membrane (Fig. 3). Thus, the 10% Ag loss was mostly from the surface, the most likely location for membrane–bacteria and membrane–virus interactions. The antimicrobial and antiviral properties of the nAg membrane were greatly reduced after leaching of Ag^+ stopped even though 90% of the added nAg remained in the membrane (Supplemental Information, Fig. S1 and Table S1). These results suggest that Ag^+ was the main antimicrobial agent.

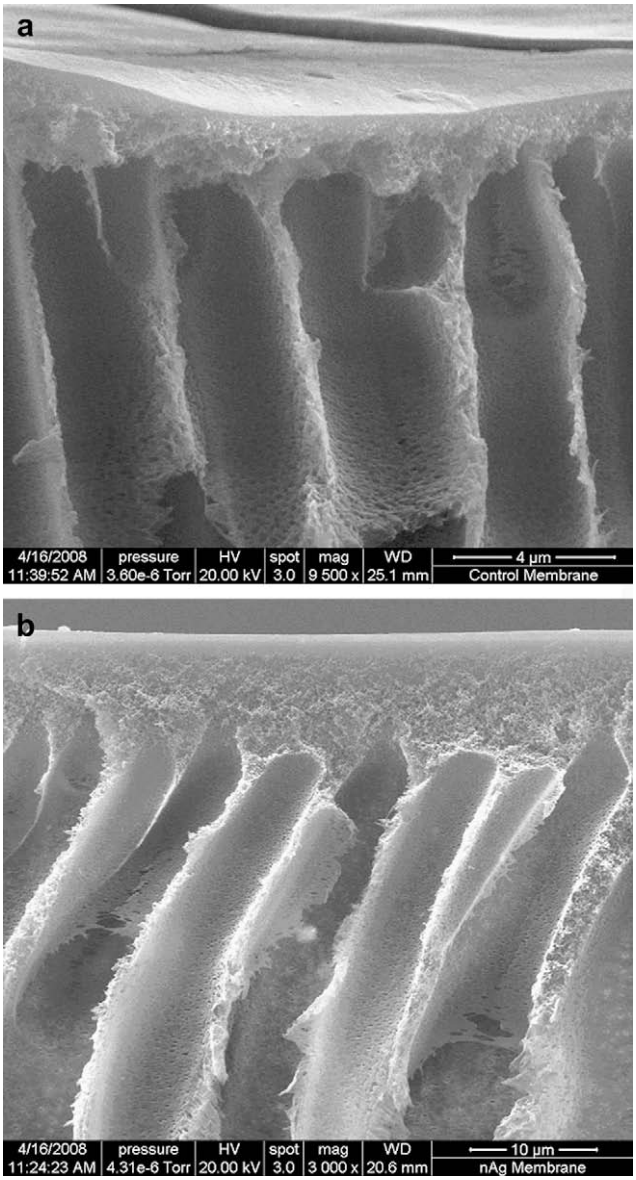

Fig. 1 – Cross-section of (a) PSf and (b) nAg–PSf membranes, taken with SEM. The addition of nAg did not change the morphology of the PSf membrane.

Table 1 – PSf and nAg–PSf membrane properties. The values are represented as average and standard deviation.

	PSf	nAg–PSf
Permeability (L/m^2/h/bar)	408 ± 180	532 ± 117
Zeta Potential at pH 7 (mV)	−6.5 ± 1.1	−6.9 ± 0.3
Hydrophobicity (Contact Angle, °)	76.8 ± 4.83	68.6 ± 6.1[a]
Thickness (mm)	0.116 ± 0.0134	0.096 ± 0.0137[a]

a Denotes significant difference at the 95% confidence interval.

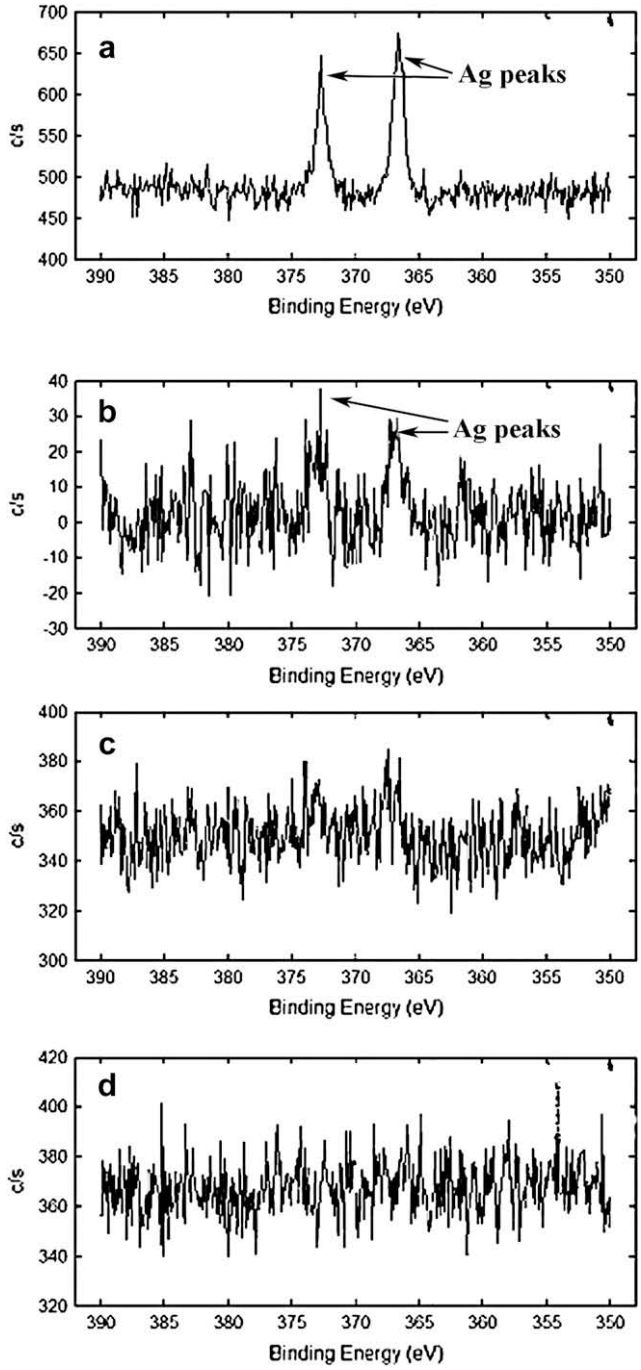

Fig. 2 – XPS analysis of silver on the surface of (a) fresh nAg–PSf membrane, (b) a nAg–PSf membrane after 1 L of DI water was filtered, (c) a nAg–PSf membrane after 4 L of DI water was filtered, and (d) a control membrane. The distinct loss in silver-related peak corresponds to a loss of silver from the membrane surface with filtration.

3.3. *Antimicrobial properties of membranes*

When a suspension of *E. coli* was filtered onto a nanosilver-containing membrane (nAg–PSf) with a dead-end filtration cell, a 2-log (99%) reduction in *E. coli* grown on the membrane surface was observed (Fig. 4a). Apparently, silver was initially

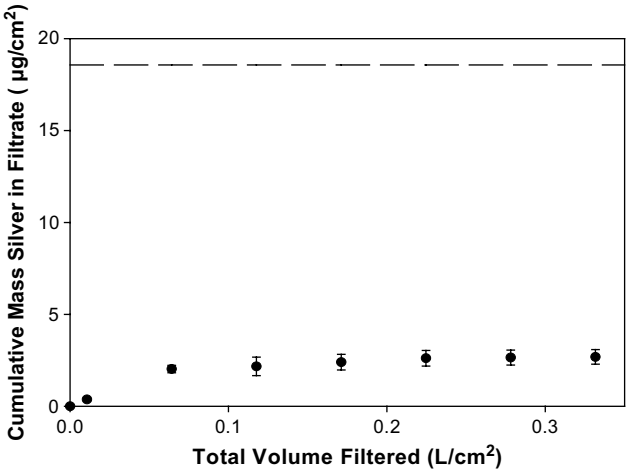

Fig. 3 – Cumulative mass of silver lost from membrane with dead-end filtration of DI water. No silver was detected in filtrate with ICP after 0.31 L/cm^2 of water was filtered. The membrane lost about 10% of total silver.

bioavailable at concentrations sufficient for *E. coli* and inactivation. Fluorescent microscopy also showed that the incorporated nAg reduced the attachment of an *E. coli* suspension to the surface of the immersed membrane coupons by 94% (Fig. 4b), most likely due to a decrease in cell viability. This significant decrease in bacteria attachment was visually apparent (Fig. 5). These two experiments infer that nAg–PSf membranes exhibit potent antimicrobial properties and are resistant to biofouling, as *E. coli* was inactivated when deposited onto the membrane surface and was less likely to attach when the membrane is exposed to a suspension of cells.

3.4. *Biofouling resistance in nAg membranes*

When biofilm formation was assessed using *P. mendocina*, very little growth (if any) was observed on the nAg membrane or in the solution surrounding the membrane (Table 2). This antimicrobial activity was attributed mainly to Ag^+ released from the membrane (see analysis of silver in the filtrate, below). Specifically, cysteine was used to bind Ag^+ and restrict its bioavailability required for killing bacteria (Fig. 6). While no growth of *E. coli* was observed in the presence of a 2.7 mg/L nAg suspension, the antimicrobial effect of silver was mitigated by the addition of 3.0 mg/L cysteine, which allowed bacterial growth. Similarly, when cysteine (27 mg/L) was placed in suspension with *P. mendocina* and the nAg–PSf membrane, the nearly 2-log inactivation of *P. mendocina* decreased to 60% (Fig. 7).

3.5. *Antiviral properties of nAg membranes*

Incorporation of nAg significantly enhanced virus removal by filtration. Influent concentrations of up to $5 \pm 0.2 \times 10^5$ PFU/mL were completely removed by filtration through nAg–PSf membranes. In contrast, viral concentrations greater than 10^2 PFU/mL were found in the filtrate of PSf membranes

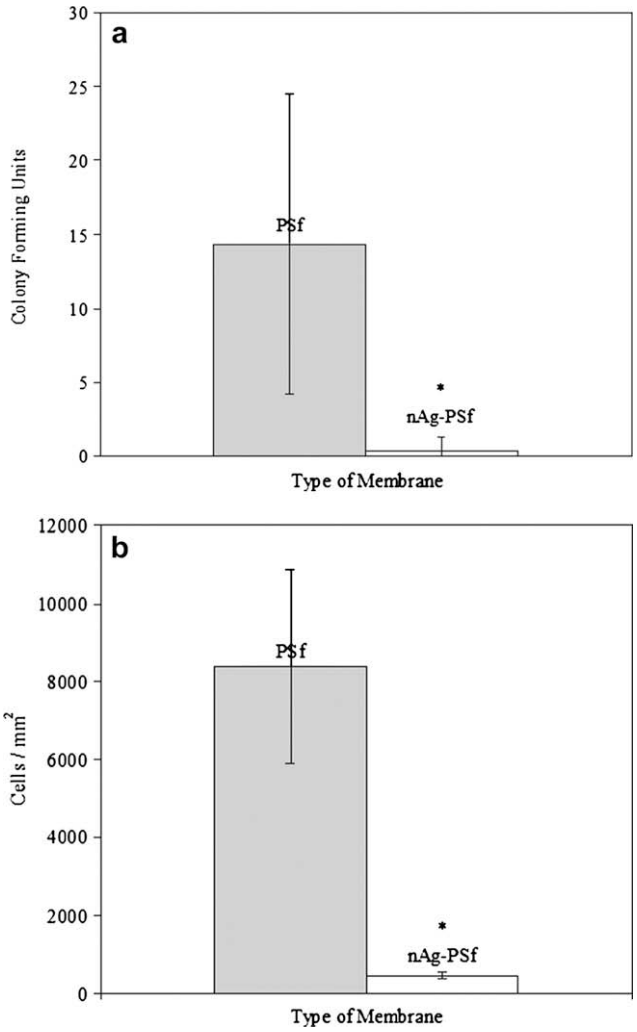

Fig. 4 – Antibacterial properties of nAg–PSf membrane. Impregnation of nAg (0.9% by weight) significantly decreased both (a) the number of *E. coli* grown on the membrane surface after filtration of a dilute bacteria suspension, as indicated by the number of colony forming units (CFU) per 9.35 cm^2 membrane coupon, and (b) the number of *E. coli* attached to the surface of a membrane coupon after 4 h incubation in a suspension of *E. coli* in MD medium. Error bars indicate 95% confidence intervals ($n = 3$).

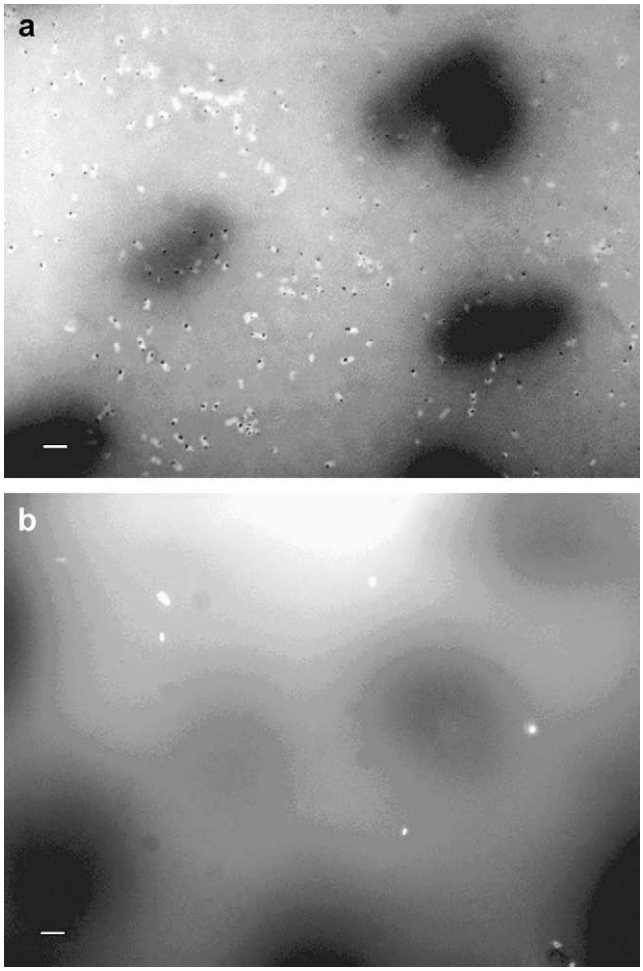

Fig. 5 – Attachment of *E. coli* suspended in MD medium to membrane surface on (a) PSf and (b) nAg–PSf membranes. Cells were stained with DAPI and viewed with a fluorescence microscope. Scale bar indicates 5 μm.

(Table 3). Although the exact mechanism of increased virus removal in this study remains unclear, various mechanisms were considered to explain virus removal, including change in membrane permeability, depth filtration, electrostatic adsorption, and inactivation of viruses by Ag^+ ions. While the nominal size of MS2 was 25 nm, our Dynamic Light Scattering (DLS) analyses indicated that the viruses were aggregated in solution, and the measured mean hydrodynamic diameter was 743 nm. Thus, it was likely that the larger aggregate size allowed some viruses to be removed by both PSf and nAg–PSf membranes through size exclusion.

Depth filtration was not a plausible cause for the increase in virus removal because the nAg–PSf membranes were thinner than the PSf controls ($p < 0.05$, Table 1). The zeta potentials of both MS2 and the membrane were negative (−18.5 mV and −7.5 mV, respectively); however, enhanced adsorption to silver oxides present in membrane may have occurred. The surface isoelectric point for silver oxides is 10.4 (Chau and Porter, 1991). Therefore, the nAg surfaces were likely positively charged at pH 8.3, the pH at which the viruses were filtered. Previous studies have reported that oxides and

Table 2 – Growth of *P. mendocina* biofilm (sessile cells) and planktonic cells during three days. Microbial concentrations are given as log(CFU/mL) with the standard deviation ($n = 3$).

	Incubation time		
	24 h	48 h	72 h
Polysulfone			
Planktonic	8.45 ± 0.13	7.68 ± 0.37	7.85 ± 0.13
Sessile	6.90 ± 0.05	6.22 ± 0.34	6.11 ± 0.58
nAg-polysulfone			
Planktonic	0.67 ± 1.35	No growth	No growth
Sessile	0.38 ± 0.76	0.5 ± 1.0	No growth

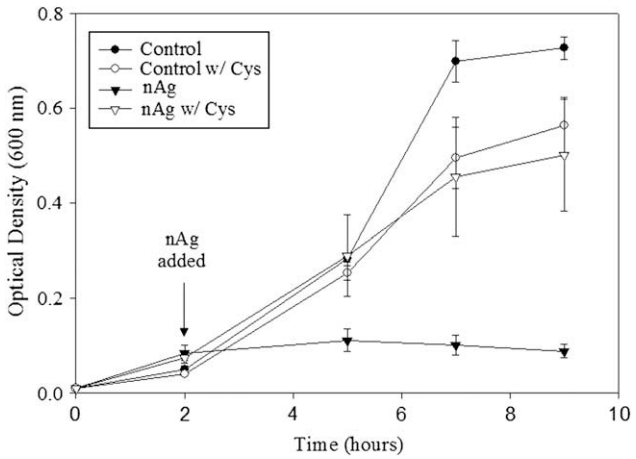

Fig. 6 – *E. coli* in suspension was inhibited by nAg (2.7 mg/L) unless cysteine (3.0 mg/L) was present. Suspension was spiked with nAg after 2 h of incubation. Error bars represent 95% confidence intervals.

hydroxides of iron and aluminum increased MS2 and poliovirus adsorption by decreasing the magnitude of negative charge at diatomaceous earth surfaces (Farrah et al., 1991). The same effect may have been responsible for the increased virus removal due to the presence of silver oxides.

In addition to localized electrostatic adsorption, inactivation and/or irreversible adsorption of viruses may have contributed to enhanced viral removal by nAg–PSf membranes (Table 3). Inactivation of MS2 viruses by Ag^+ ions has been previously reported (Kim et al., 2008) and was corroborated in additional batch tests with a suspension of MS2 (10^9 PFU/mL) (Supplemental Information, Table S2). Interestingly, Ag^+ ions (18 mg/L) exerted significantly stronger antiviral activity (4-log removal after 1.5 h exposure) than an equivalent concentration of nAg particles, which released only 8 μg/L Ag^+ ions,

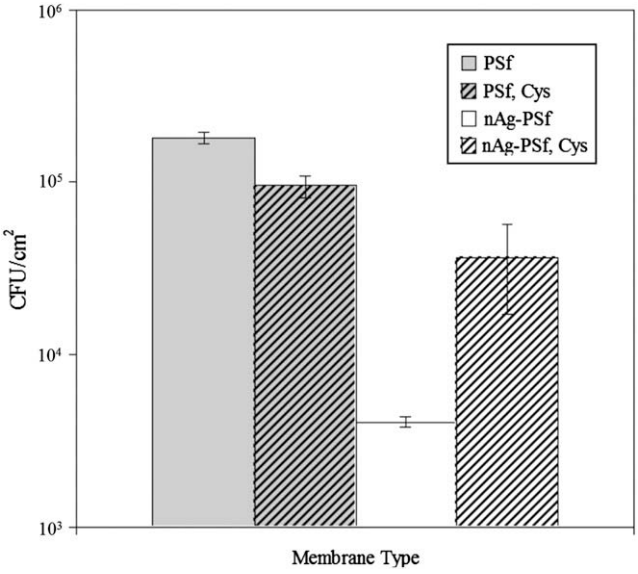

Fig. 7 – Inhibition of *P. mendocina* KR1 biofilm by nAg–PSf was prevented by 27 mg/L cysteine (cys). This graph depicts biofilm growth after 4 h incubation in MD medium.

Table 3 – Viral removal by membrane filtration. Plaque counts were performed on the influent and filtrates through PSf and nAg–PSf membranes. The values are expressed as average and standard deviation ($n = 4$).

Influent (PFU/mL)	PSf filtrate (PFU/mL)	nAg–PSf filtrate (PFU/mL)
$5 \pm 0.2 \times 10^5$	625 ± 35	0
$6 \pm 0.1 \times 10^4$	375 ± 148	0

causing no significant virus inactivation. This suggests that Ag^+ released from nAg may have accounted for some enhanced removal.

3.6. *Technological challenges*

Silver release from commercial products containing nAg is an ever-growing concern (Benn and Westerhoff, 2008). This calls for future research that leads to improved nAg incorporation protocols that ideally concentrate the particles on the selective layer of the membrane, anchoring or coating nAg to slow the release of silver ions. Potential approaches to be explored include encapsulating nAg in a polymer and then covalently binding it to membrane polymers either directly or through the use of cross-linkers. Another option may be to encapsulate the silver in a substance that is degraded by bacteria so it is released at a constant rate (Loher et al., 2008). Additionally, silver lost from the membrane could be regenerated through the reduction and deposition of silver salts, such as $AgNO_3$ (Deng et al., 2008).

In addition to rapid loss of silver from these membranes, future use of these membranes in water treatment must address two other potential challenges with membrane performance – bacterial resistance to heavy metals and water chemistry. To illustrate the first challenge, similar experiments were conducted with *P. aeruginosa*, a metal-resistant bacterium that contains a cation-antiporter efflux pump (Hassen et al., 2001) that showed no decreases in bacteria growth (Fig. S2). It is also very likely that the effectiveness of nAg–PSf membranes will be influenced by the composition of the water to which they are exposed. Silver toxicity to *E. coli* is altered by common water constituents that affect silver solubility and bioavailability, such as chloride, phosphates, sulfides, and compounds containing thiol groups. These compounds decrease the potency of silver ions and, in the case of cysteine, can reverse some of the damage to bacteria cells caused by silver (Russell and Hugo, 1994; Gupta and Silver, 1998). Bactericidal action of silver ions also increases with increasing temperature and pH (Russell and Hugo, 1994), which are two important factors in water treatment process control.

4. Conclusions

The use of silver-impregnated antimicrobial materials is widespread, and the potential for silver to solve the biofouling problem in water filtration membranes is worthy of

consideration. We show in this study that nAg–PSf membranes were effective against two strains of bacteria – *E. coli* K12 and *P. mendocina* KR1, and that the antimicrobial activity was primarily due to the release of Ag^+ ions. Not only were these membranes antimicrobial, but they also prevented bacteria attachment to the membrane surface and reduced biofilm formation. Additionally, nAg–PSf membranes showed a significant improvement in virus removal.

In order to take advantage of nAg-enhanced membrane properties, nAg does not need to be embedded during the membrane preparation process. It can be added to a commercial membrane and regenerated as needed. However, two significant challenges to long-term performance of nAg-embedded membranes were apparent: loss of antimicrobial and antiviral activity due to depletion of silver from the membrane surface and ineffectiveness against silver-resistant bacterial strains. Rapid silver depletion could be addressed by future research focusing on better nAg fixation techniques that concentrate the silver near the surface of the membrane (where it is most effective) and encapsulate the silver to slow the release rate. Because eventual silver depletion may be unavoidable, the effectiveness of nAg regeneration by reductive deposition of silver salts should be further explored (Chou et al., 2005; Deng et al., 2008). While nAg-impregnated membranes would not guarantee protection against silver-resistant bacteria strains, they may ensure antimicrobial activity against a wide variety of bacteria and viruses and provide long-term protection against biofouling and viral penetration of water filtration membranes.

Acknowledgements

The authors thank EPA-STAR R832534 and the NSF-funded Center for Biological and Environmental Nanotechnology for financial support, Zoltan A. Krudy and Mark Hoffman for help in the laboratory, and Erika Bryant for TEM analysis.

Appendix. Supplementary data

Supplementary data associated with this article can be found in the online version, at doi:10.1016/j.watres.2008.11.014

REFERENCES

Bellara, S.R., Cui, Z.F., MacDonald, S.L., Pepper, D.S., 1998. Virus removal from bioproducts using ultrafiltration membranes modified with latex particle pretreatment. Bioseparation 7, 79–88.

Benn, T.M., Westerhoff, P., 2008. Nanoparticle silver released into water from commercially available sock fabrics. Environmental Science and Technology 42, 4133–4139.

Bosetti, M., Masse, A., Tobin, E., Cannas, M., 2002. Silver coated materials for external fixation devices: in vitro biocompatibility and genotoxicity. Biomaterials 23, 887–892.

Chau, L.K., Porter, M.D., 1991. Surface isoelectric point of evaporated silver films – determination by contact-angle titration. Journal of Colloid and Interface Science 145, 283–286.

Cheryan, M., 1998. Ultrafiltration and Microfiltration Handbook, vol. xvii. Technomic Pub. Co., Lancaster, PA, 527 p.

Chou, W.L., Yu, D.G., Yang, M.C., 2005. The preparation and characterization of silver-loading cellulose acetate hollow fiber membrane for water treatment. Polymers for Advanced Technologies 16, 600–607.

Cunningham, J.H., Cunningham, C., Van Aken, B., Lin, L.S., 2008. Feasibility of disinfection kinetics and minimum inhibitory concentration determination on bacterial cultures using flow cytometry. Water Science and Technology 58, 937–944.

Damm, C., Munsted, H., Rosch, A., 2007. Long-term antimicrobial polyamide 6/silver-nanocomposites. Journal of Materials Science 42, 6067–6073.

Davies, R.L., Etris, S.F., 1997. The development and functions of silver in water purification and disease control. Catalysis Today 36, 107–114.

Deng, Y.Q., Dang, G.D., Zhou, H.W., Rao, X.H., Chen, C.H., 2008. Preparation and characterization of polyimide membranes containing Ag nanoparticles in pores distributing on one side. Materials Letters 62, 1143–1146.

Elechiguerra, J.L., Burt, J.L., Morones, J.R., Camacho-Bragado, A., Gao, X., Lara, H.H., Yacaman, M.J., 2005. Interaction of silver nanoparticles with HIV-1. Journal of Nanobiotechnology 3, 6.

Farrah, S.R., Preston, D.R., Toranzos, G.A., Girard, M., Erdos, G.A., Vasuhdivan, V., 1991. Use of modified diatomaceous – earth for removal and recovery of viruses in water. Applied and Environmental Microbiology 57, 2502–2506.

Feng, Q.L., Wu, J., Chen, G.Q., Cui, F.Z., Kim, T.N., Kim, J.O., 2000. A mechanistic study of the antibacterial effect of silver ions on *Escherichia coli* and *Staphylococcus aureus*. Journal of Biomedical Materials Research 52, 662–668.

Fievet, P., Sbai, M., Szymczyk, A., Vidonne, A., 2003. Determining the zeta-potential of plane membranes from tangential streaming potential measurements: effect of the membrane body conductance. Journal of Membrane Science 226, 227–236.

Gogoi, S.K., Gopinath, P., Paul, A., Ramesh, A., Ghosh, S.S., Chattopadhyay, A., 2006. Green fluorescent protein-expressing *Escherichia coli* as a model system for investigating the antimicrobial activities of silver nanoparticles. Langmuir 22, 9322–9328.

Gupta, A., Silver, S., 1998. Silver as a biocide: will resistance become a problem? Nature Biotechnology 16, 888.

Hassen, A., Jerboui, Z., Cherif, M., Saidi, N., Gharbi, S., Boudabous, A., 2001. Impact of heavy metals on the selective phenotypical markers of *Pseudomonas aeruginosa*. Microbial Ecology 42, 99–107.

Jayasekara, N.Y., Heard, G.M., Cox, J.M., Fleet, G.H., 1999. Association of micro-organisms with the inner surfaces of bottles of non-carbonated mineral waters. Food Microbiology 16, 115–128.

Kang, S.W., Kim, J.H., Char, K., Won, J., Kang, Y.S., 2006. Nanocomposite silver polymer electrolytes as facilitated olefin transport membranes. Journal of Membrane Science 285, 102–107.

Kaye, G.W.C., Laby, T.H., 1986. Tables of Physical and Chemical Constants and Some Mathematical Functions. Longman, London, New York.

Kennedy, J.E., Wei, C.I., Oblinger, J.L., 1986. Methodology for enumeration of coliphages in foods. Applied and Environmental Microbiology 51, 956–962.

Kim, J.Y., Lee, C., Cho, M., Yoon, J., 2008. Enhanced inactivation of *E. coli* and MS2 phage by silver ions combined with UV-A and visible light irradiation. Water Research 42, 356–362.

Li, Q., Mahendra, S., Lyon, D.Y., Brunet, L., Liga, M.V., Li, D., Alvarez, P.J.J., 2008. Antimicrobial nanomaterials for water

disinfection and microbial control: potential applications and implications. Water Research 42 (18), 4591–4602.
Liau, S.Y., Read, D.C., Pugh, W.J., Furr, J.R., Russell, A.D., 1997. Interaction of silver nitrate with readily identifiable groups: relationship to the antibacterial action of silver ions. Letters in Applied Microbiology 25, 279–283.
Loher, S., Schneider, O.D., Maienfisch, T., Bokorny, S., Stark, W.J., 2008. Micro-organism-triggered release of silver nanoparticles from biodegradable oxide carriers allows preparation of self-sterilizing polymer surfaces. Small 4, 824–832.
Mcdonogh, R., Schaule, G., Flemming, H.C., 1994. The permeability of biofouling layers on membranes. Journal of Membrane Science 87, 199–217.
Morones, J.R., Elechiguerra, J.L., Camacho, A., Holt, K., Kouri, J. B., Ramirez, J.T., Yacaman, M.J., 2005. The bactericidal effect of silver nanoparticles. Nanotechnology 16, 2346–2353.
Mulder, M., 1990. Basic Principles of Membrane Technology. Kluwer Academic Publishers, Norwell, MA, U.S.A.
de Prijck, K., Nelis, H., Coenye, T., 2007. Efficacy of silver-releasing rubber for the prevention of *Pseudomonas aeruginosa* biofilm formation in water. Biofouling 23, 405–411.
Pal, S., Tak, Y.K., Song, J.M., 2007. Does the antibacterial activity of silver nanoparticles depend on the shape of the nanoparticle? A study of the gram-negative bacterium *Escherichia coli*. Applied and Environmental Microbiology 73, 1712–1720.
Panacek, A., Kvitek, L., Prucek, R., Kolar, M., Vecerova, R., Pizurova, N., Sharma, V.K., Nevecna, T., Zboril, R., 2006. Silver colloid nanoparticles: synthesis, characterization, and their antibacterial activity. Journal of Physical Chemistry B 110, 16248–16253.
Ratte, H.T., 1999. Bioaccumulation and toxicity of silver compounds: a review. Environmental Toxicology and Chemistry 18, 89–108.
Ridgway, H., Ishida, K., Rodriguez, G., Safarik, J., Knoell, T., Bold, R., 1999. Biofouling of membranes: membrane preparation, characterization, and analysis of bacterial adhesion. Biofilms 310, 463–494.
Russell, A.D., Hugo, W.B., 1994. Antimicrobial activity and action of silver. Progress in Medicinal Chemistry 31, 351–370.
Savage, N., Diallo, M.S., 2005. Nanomaterials and water purification: opportunities and challenges. Journal of Nanoparticle Research 7, 331–342.
Silver, S., Phung, L.T., 1996. Bacterial heavy metal resistance: new surprises. Annual Review of Microbiology 50, 753–789.
Sondi, I., Salopek-Sondi, B., 2004. Silver nanoparticles as antimicrobial agent: a case study on *E. coli* as a model for Gram-negative bacteria. Journal of Colloid and Interface Science 275, 177–182.
Trevors, J.T., 1987. Silver resistance and accumulation in bacteria. Enzyme and Microbial Technology 9, 331–333.
WHO, 2004. Guidelines for Drinking Water Quality. World Health Organization, Geneva, Switzerland.
Xu, X.H., Brownlow, W.J., Kyriacou, S.V., Wan, Q., Viola, J.J., 2004. Real-time probing of membrane transport in living microbial cells using single nanoparticle optics and living cell imaging. Biochemistry 43, 10400–10413.
Zhu, B.T., Clifford, D.A., Chellam, S., 2005. Virus removal by iron coagulation-microfiltration. Water Research 39, 5153–5161.